

A method for optical snow-cover mapping in sparse forest

Dagrun Vikhamar¹ and Rune Solberg²

¹Department of Physical Geography, University of Oslo, P.O. Box 1042 Blindern, N-0316 Oslo, Norway
E-mail: dagrun.vikhamar@geografi.uio.no; Phone: +47-2285-5804; Fax: +47-2285-7230

²Norwegian Computing Center, P.O. Box 114 Blindern, N-0314 Oslo, Norway
E-mail: rune.solberg@nr.no; Phone: +47-2285-2500; Fax: +47-2269-7660

ABSTRACT

A snow-cover mapping method for sparse forest by optical remote sensing is proposed. The method is based on linear sub-pixel reflectance modeling of the surface components snow, individual tree species, tree shadows and bare ground. Experiments are performed using a 100% snow-covered Landsat TM scene and aerial photos covering spruce, pine and birch forest in the Jotunheimen mountain area of South Norway. The results show that sub-pixel modeling of snow in sparse forest is possible, but effects of topography and direct and diffuse illumination, which influence the reflectance variability, should be accounted for to improve the results.

INTRODUCTION

Seasonal snow may cover up to 50 million km² of the Earth's land surface [1]. Most of the seasonal snow is located in the Northern Hemisphere. The boreal forest is seasonally snow-covered and covers 12 million km² of the land surface. Seasonally snow-covered forest is also present in high mountain regions of temperate latitudes.

Monitoring the snow-cover extent is important both for climatological studies and for hydrological applications. Due to the high snow albedo and emissivity of snow compared to other natural surfaces, variations in the global snow-cover distribution affect the global energy balance. Hydrological applications include support to hydropower production planning and river flood predictions.

Several classification methods have been developed or adapted to optical snow-cover mapping, e.g. the SNOMAP-algorithm [2], linear spectral unmixing [3], and an empiric linear sub-pixel classification method [4]. The classification methods give reasonable results for unforested areas, see e.g. [2]. However, forested areas constitute a problem due to the trees' contributed radiance, in addition to reducing the radiance from the snow below the trees. Classification methods generally underestimate the snow cover in forest, see e.g. [5]. The SNOMAP-algorithm has been extended by including the Normalized Difference Vegetation Index to map snow-covered forest [6], and verification of the algorithm is investigated by [7].

The objective of this work is to study the possibilities for determining the snow coverage at sub-pixel level in sparse forest by optical remote sensing. A snow-cover mapping method, based on linear sub-pixel reflectance modeling, is proposed. Experiments focus on physical models of the forest in order to understand how the various effects influence the pixel reflectance, and with the aim to derive a simplified

operational model from a physical model. Results from experiments for spruce, pine and birch forest, and mixed pine and birch forest are presented and discussed. The experiments deal with situations of 100% snow coverage, while less than 100% snow coverage will be investigated in a later work.

SPARSE FOREST SNOW-COVER MAPPING METHOD

The satellite measured radiance above a snow-covered forest during the snowmelt season is influenced by a number of scene components, illumination- and atmospheric effects. The main scene components of a snow-covered forest are the surface covers trees, snow and bare ground. The spectral radiance of each surface cover is affected by the temporal natural variability of the surface cover and the topography. Based on the influence of the variation in radiance due to temporal natural variability, a ranking of the scene components is proposed. Snow is temporally the most unstable surface component. Due to the continuous snow metamorphoses, which changes the snow physical properties, the albedo may vary between 35% and 90%. [1]. Bare ground consists of vegetation, vegetation litter, rocks and soils. Bare ground is ranked as the second most influencing surface component provided that the vegetation is non-green and the temporal moisture conditions are stable. Non-green deciduous trees, conifers and topography are the least changing surface components, giving the most stable influence on the radiance. Added to these components are the illumination effects, which are due to direct and diffuse sunlight, individual trees (shadowed tree crowns, shadowed snow and mutual shadowing) and topography. Topography alters the areas covered by shadows.

A linear sub-pixel reflectance model, which is an area-weighted sum of the surface components, is chosen for the modeling:

$$R = A_P R_P + A_S R_S + A_B R_B + A_{SW} R_{SW} + A_{SWP} R_{SWP} + A_{SWS} R_{SWS} + A_{SWB} R_{SWB} + A_{BG} R_{BG},$$

where R is the pixel reflectance, A_P , A_S , A_B are the area proportions of a pixel covered by pine, spruce and birch tree crowns, respectively. A_{SW} and A_{BG} represent the area proportions covered by illuminated snow and bare ground, respectively. R_P , R_S , R_B are the tree-crown reflectances of pine, spruce and birch, respectively. R_{SW} is the illuminated snow reflectance, while R_{BG} is the bare ground reflectance. Shadows within the tree crowns are included in the model by using tree-crown reflectances representing both illuminated and shadowed tree crowns. A shadowed snow component for pine (A_{SWP} , R_{SWP}), spruce (A_{SWS} , R_{SWS}) and birch (A_{SWB} , R_{SWB})

models the shadows on the snow. Spruce and pine tree crowns are assumed opaque, while leafless birch tree crowns are transparent with a contributing reflectance from the areas below the tree crowns. The birch tree crown reflectance (R_B) is modeled separately using a linear mixing reflectance model of illuminated snow and estimated effective branch area proportion (the proportion of birch branches within a tree crown when projected on the ground). The effective branch area proportion (A_B') is estimated with tree height (TH) as input parameter to the regression function $A_B' = aTH + b$. Similarly, the effective shadow area proportion (A_{SWB}') is estimated from the tree height (TH): $A_{SWB}' = cTH + d$. These functions are determined empirically using field measured spectral signatures of entire tree crowns, single branches and shadows of birch trees of variable heights.

The model assumes that the ground area covered by a pixel is greater than the size of individual trees. Other assumptions concerning a snowmelt season are constant tree-crown reflectance for a given solar elevation angle, snow-free tree crowns and constant area covered by tree crowns.

DATA SET

A study area with maximum 10° terrain slope in the Joutunheimen mountain area of South Norway (9°E , 61°N , 900 m.a.s.l.) covering spruce, pine and birch forest was selected for experiments. Infrared aerial photos (1:15,000) from August 1998 were used as reference data for a 100% snow-covered Landsat TM scene from 21 April 1998. A forest model representation was generated by high precision photogrammetrical measurements of individual trees. Tree species, tree height, tree-crown diameter and position were measured for each tree. In total 14,511 birch trees, 13,611 pine trees and 1652 spruce trees were measured. These data served to generate crown coverage maps for each tree species of Landsat TM spatial resolution. Shadow maps were generated by calculating the shadowed ground area of each tree based on its tree height, tree crown diameter, the solar elevation angle, the solar azimuth angle and modeling the trees as cylinders with spherical top. Sub-areas of the Landsat TM image were geometrically corrected using coordinates from the aerial photos. The satellite image pixel values were calibrated to reflectance using spectral signature of tap water [8] and in-situ field measured snow spectral signatures. The calibration eliminated TM5 and TM7 due to low water and snow reflectance. TM1 was excluded due to pixel saturation from high snow reflectance.

EXPERIMENTS

The experiments in the work described here focus on situations with 100% snow coverage, thus the bare ground component is eliminated. This is to reduce the number of effects in this first approach. The following data sets were analyzed: 1. Snow and pine forest (762 pixels); 2. Snow and spruce forest (153 pixels); 3. Snow and birch forest (467 pixels); and 4. Snow and mixed pine and birch forest (607 pixels). The number of pixels covering other mixtures of tree species was too low for statistical analysis. As a first

approach the snow was modeled totally illuminated for data sets 1-4. TM2-4 reflectance values were simulated from field-measured spectral signatures of snow, spruce tree crowns, pine tree crowns and branches of birch trees (Tab. 1). Reflectance of birch branches was calculated by a solar elevation adjusted mixture of illuminated and shadowed branch spectral signatures. The aerial-photo-derived crown coverage map constituted the area proportions of pine, spruce and birch tree crowns (A_p , A_s , A_b).

In a second approach, shadowed snow from single tree species was included by integrating a shadowed snow component for each tree species. The generated shadow maps constituted the shadowed area proportions (A_{SWP} , A_{SWS} , A_{SWB}). TM2-4 reflectance values were derived from field measured spectral signatures of shadowed snow from individual pine, spruce and birch trees (Tab. 1). The applied regression functions for determining the effective birch branch area proportion and the effective shadow area proportion was: $A_B' = 4.7 TH + 2.05$ and $A_{SWB}' = 3.9 TH + 16.8$. The average tree height (TH) for single TM pixels were input to the regression functions. The results from the modeling without shadows, and with shadows, were evaluated against the measured Landsat TM reflectance (Fig. 1, Tab. 2). Measured TM2-4 reflectance were highly correlated ($R^2=0.97-0.99$), therefore only TM3 is presented.

RESULTS

Comparing the measured and modeled Landsat TM reflectance shows as expected a general tendency of reduced reflectance with increasing crown coverage for all data sets. Integrating the shadows considerably improved the regression functions for measured and modeled reflectance for all data sets (Tab. 2). For the data sets with single tree species, the snow and pine forest shows the best model fit by

Tab. 1: Simulated mean TM2-4 reflectance for the surface components used in the reflectance modeling.

Surface component	TM2	TM3	TM4
Illuminated snow (R_{sw})	92	89	77
Pine tree crowns (R_p)	12	7	47
Spruce tree crowns (R_s)	10	6	48
Birch branches (R_b')	10	11	23
Pine, shadowed snow (R_{SWP})	14	9	8
Spruce, shadowed snow (R_{SWS})	20	17	16
Birch, shadowed snow (R_{SWB})	26	21	16

Tab. 2: Estimated regression parameters from measured and modeled Landsat TM3 reflectance.

Data set number	Slope	Interception	R^2
1. Illuminated snow	0.33	66.85	0.50
1. Shadowed snow	1.14	2.16	0.54
2. Illuminated snow	0.07	80.85	0.26
2. Shadowed snow	0.44	39.71	0.45
3. Illuminated snow	0.15	76.15	0.35
3. Shadowed snow	0.48	48.17	0.58
4. Illuminated snow	0.24	70.51	0.43
4. Shadowed snow	0.95	13.5	0.55

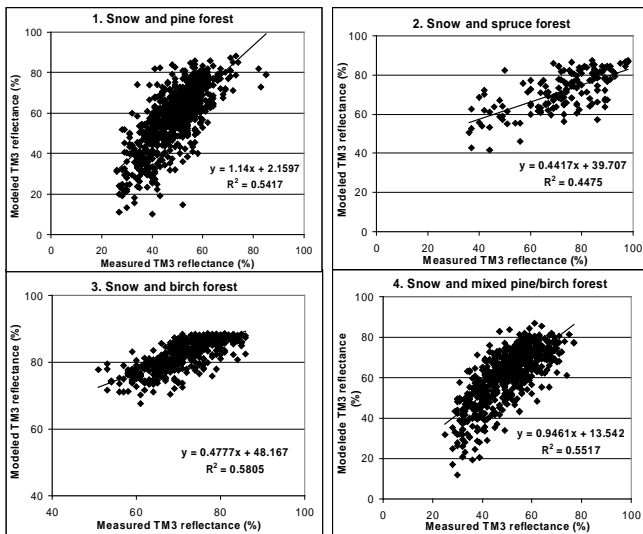


Fig. 1: Measured and modeled Landsat TM3 reflectance for the data sets 1-4 with tree shadows included.

approaching the slope 1 and intercept 0. The data set covers a pine forest composed of a very sparse forest (0-12% crown coverage) and a denser forest (0-30% crown coverage). The mean crown coverage is 7.4%. Data set 2, snow and spruce forest, shows an improved result when including shadows, but still the model greatly overestimates the reflectance. The crown coverage varies between 0-12%, with 3.9% mean crown coverage. Modeling the very sparse pine forest separately shows a similar overestimation of reflectance. Including denser spruce forest would likely improve the model. Unfortunately, cumulus clouds in the Landsat TM-scene occupied areas with dense spruce forest. Data set 3, snow and birch forest, considerably improves the results when including shadows, although the model still overestimates the reflectance. Crown coverage varies from 0-34% with 7.8% mean crown coverage. Data set 4, snow and mixed pine and birch forest, models the reflectance quite well when shadows are included. Pine and birch crown coverage varies between 0-27% and 0-30%, respectively. Mean pine and birch crown coverage are 6.4% and 4.0%. Typically, pixels with high reflectance have low crown coverage of both pine and birch, while low reflectance is associated with high pine crown coverage.

DISCUSSION AND CONCLUSIONS

The importance of including shadows in the models was demonstrated through the improved results for all tree species. Shadows cover great areas in a sparse forest when solar elevation is modest. Including other effects affecting the amounts of direct and diffuse illumination in forest may reduce the large scattering in the models. Increased crown coverage reduces the diffuse illumination of the snow, and increases the effect of mutual shadowing from surrounding trees. Single trees get increased areas of shadowed branches with increasing crown density. Accounting for topographically induced shadow effects will also improve the

modeling. Outliers of the pine forest model are located at a forest limit between sparse and denser pine forest, thus indicating that sub-pixel displacement of the coregistration of the Landsat TM-scene may improve the model results. Further work will be performed to quantify and integrate these effects in the models.

The results from the physical modeling will be exploited to develop a simplified operational model. An operational model will be based on retrieving the necessary forest parameters (crown coverage, tree height, tree species) from existing forest maps, supplied by a spectral library of tree crowns, snow and bare ground spectral signatures. Dense conifer forest may be applied as control areas for detecting whether intercepted snow is present in the tree crowns. Intercepted snow changes the tree-crown reflectance and has to be taken into account.

ACKNOWLEDGMENTS

This work was supported by SNOWTOOLS, an environment and climate project, funded by the Commission of the European Communities, contract no. ENV4-CT96-0304, and the Department of Geography, University of Oslo, Norway.

REFERENCES

- [1] D.L. Hartmann, *Global Physical Climatology*, Academic Press, 411 p., 1994.
- [2] D.K. Hall, G.A. Riggs, and V.V. Salomonsen, "Development of methods for mapping global snow cover using Moderate Resolution Imaging Spectroradiometer Data", *Remote Sensing of Environment*, vol. 54, pp. 127-140, 1995.
- [3] A.W. Nolin, J. Dozier and L.A.K. Mertes, "Mapping alpine snow using a spectral mixture modeling technique", *Annals of Glaciology*, vol. 17, pp. 121-124, 1993.
- [4] R. Solberg and T. Andersen, "An automatic system for operational snow-cover monitoring in the Norwegian mountain regions", *Proceedings of IGARSS'94 Symposium*, Pasadena, California, USA, pp. 2084-2086, August 1994.
- [5] R. Solberg, D. Hiltbrunner, J. Koskinen, T. Guneriussen, K. Rautiainen and M. Hallikainen, *Snow algorithms and products - Review and recommendations for research and development*, Project SNOWTOOLS WP 410, NR Report No. 924, Norwegian Computing Center, Oslo, 111 p., December 1997.
- [6] D.K. Hall, J.L. Foster, D.L. Verbyla, A.G. Klein, and C.S. Benson, "Assessment of snow-cover mapping accuracy in a variety of vegetation-cover densities in Central Alaska", *Remote Sensing of Environment*, vol. 66, pp. 129-137, 1998.
- [7] A.G. Klein, D.K. Hall, and G.A. Riggs, "Improving snow-cover mapping in forests through the use of a canopy reflectance model", *Hydrological Processes*, vol. 12, pp. 1723-1744, 1998.
- [8] The Johns Hopkins University Spectral Library. <http://speclib.jpl.nasa.gov/>